

# A Tractable Product Channel Model for Line-of-Sight Scenarios

U. Fernandez-Plazaola, L. Moreno-Pozas, F. J. Lopez-Martinez,  
J. F. Paris, E. Martos-Naya and J. M. Romero-Jerez

**Abstract**—We here present a general and tractable model for line-of-sight (LOS) scenarios, which is based on the product of two independent and non-identically distributed  $\kappa\text{-}\mu$  shadowed random variables. Simple closed-form expressions for the probability density function, cumulative distribution function and moment-generating function are derived, which are as tractable as the corresponding expressions derived from a product of Nakagami- $m$  random variables. This model simplifies the challenging characterization of LOS product channels, as well as combinations of LOS with non-LOS ones. It also shows a higher flexibility when fitting measurements with respect to exact approaches based on the Rician distribution.

**Index Terms**—Backscatter communications, fading channels,  $\kappa\text{-}\mu$  shadowed fading, product channel, statistics, wireless powered communications.

## I. INTRODUCTION

The statistical characterization of products of random variables (RVs) plays an important role in a wide range of applications, including statistical testing [1], hydrology [2], cosmology [3] and wireless communications [4]. Even for the simplest case where only two RVs are considered, i.e.  $Z = XY$ , with  $X$  and  $Y$  being independent, the statistical characterization of  $Z$  is usually much more involved than the individual distributions of  $X$  and  $Y$ .

In wireless communications,  $Z$  is generally referred to as *product channel*, which is related to a product of two random processes associated with the stochastic nature of wireless communication channels. The product channel naturally arises in the context of communication systems assisted by relays [5], when modeling propagation effects such as keyholes [6], diffraction [7] and composite fading [8], or turbulence-induced scintillation in free-space optical communications [9]. Further scenarios on which the product channel characterization is essential also include wireless powered communications (WPC) [10–12] and backscatter communications [13, 14]. Thus, the statistical characterization of the product channel is of paramount relevance for understanding the performance

U. Fernandez-Plazaola, L. Moreno-Pozas, F. J. Lopez-Martinez, J. F. Paris, and E. Martos-Naya are with Dpto. Ingeniería de Comunicaciones, Universidad de Málaga, Málaga 29071, Spain. E-mail: [>{unai,imp,fjlopezm,paris,eduardo}@ic.uma.es](mailto:{unai,imp,fjlopezm,paris,eduardo}@ic.uma.es). J. M. Romero-Jerez is with Dpto. Tecnología Electrónica, Universidad de Málaga, Málaga 29071, Spain. E-mail: [romero@dte.uma.es](mailto:romero@dte.uma.es).

This work has been funded by the Consejería de Economía, Innovación, Ciencia y Empleo of the Junta de Andalucía, the Spanish Government and the European Fund for Regional Development FEDER (projects P2011-TIC-7109, P2011-TIC-8238 and TEC2014-57901-R). This work has been submitted to the IEEE for possible publication. Copyright may be transferred without notice, after which this version may no longer be accessible.

limits of wireless communication systems operating in these scenarios, either in line-of-sight (LOS) or non-LOS (NLOS) propagation conditions.

Taking a deeper look into the literature, one alternative in many scenarios boils down to approximating the resulting product channel as a product of two NLOS fading channels [10–14] regardless of the propagation conditions. The main motivation behind this approach is defining a tractable framework, since the characterization of LOS product (or LOSxLOS) channels is very challenging and cannot be given in closed-form, but in terms of double infinite sums of special functions [15]. Therefore, for the sake of tractability, some authors have approximated both LOS links as NLOS ones, which have closed-form characterization [5, 7]. Indeed, using the Nakagami- $m$  distribution for approximating the Rician distribution is a classical approach which can simplify the characterization of some scenarios [16, 17]. In other scenarios, however, despite being simple and insightful, the results derived therein can give inaccurate approximations when the propagation conditions are clearly LOS. Moreover, the approximation of the Rician distribution through a Nakagami- $m$  distribution has severe limitations related to the different diversity order of such distributions [18]; this is especially relevant in the high signal-to-noise-ratio (SNR) regime, which is of key importance when analyzing system performances. Intermediate models, which only approximate one of the two LOS links, can give simpler results when compared to the exact characterization of Rician product channels, although the resulting statistical characterization is still complicated, since its cumulative distribution function (CDF) involves an infinite sum of Meijer  $G$ -functions [19, eq. (23)].

With all these considerations, the literature is lacking from LOS product channel models which are analytically tractable. Since the complexity of previous results for LOS product channel models are mainly due to the challenge posed by considering a product of two Rician RVs, we here propose to characterize product channels by means of a more general distribution, which in turn will help simplifying the problem. We will introduce a product channel model based on the  $\kappa\text{-}\mu$  shadowed fading distribution [20, 21] and built as the product of two independent and non-identically distributed (INID)  $\kappa\text{-}\mu$  shadowed RVs with integer fading parameters, which includes the Rician product model as a special case. For the sake of shorthand notation, we will refer to this new fading distribution as the  $\mathcal{P}$ -distribution (where  $\mathcal{P}$  stands for product). Although we here focus on simplifying the analysis of Rician product channels, the results here presented for the  $\kappa\text{-}\mu$  shadowed

product channel can unify the analysis of a vast set of product models as special cases, including LOSxLOS product channel based on the  $\kappa\text{-}\mu$  distribution, as well as LOSxNLOS and NLOSxNLOS product channels based on the  $\eta\text{-}\mu$ , Nakagami- $m$  and Rayleigh distributions [22]. The usefulness of this new distribution, both in terms of tractability and improved fit to field measurements, is exemplified in the contexts of WPC and backscatter communications.

The remainder of this paper is structured as follows. The chief probability functions of the  $\mathcal{P}$ -distribution is introduced in Section II. Then, the application of this distribution to two scenarios of interest is addressed in Sections III and IV: WPC and backscatter communications, respectively. Finally, main conclusions are drawn in Section V.

## II. STATISTICAL CHARACTERIZATION

In this section we will derive the chief probability functions characterizing the  $\mathcal{P}$ -distribution, which is built from the product of two INID  $\kappa\text{-}\mu$  shadowed RVs. Throughout this paper, we will consider the distributions associated to the power envelope in  $\kappa\text{-}\mu$  shadowed fading channels (or equivalently, the instantaneous receive SNR  $\gamma$ ). The distribution of the received signal envelope  $r$  can be easily computed through a simple change of variables, assuming that  $\gamma \propto r^2$ .

### A. Preliminary results

We will first present some preliminary results that will become relevant for the following derivations.

*Lemma 1 (The  $\kappa\text{-}\mu$  shadowed distribution with integer fading parameters [23]):* Let  $\gamma$  be a  $\kappa\text{-}\mu$  shadowed random variable with mean  $\bar{\gamma}$  and shape parameters  $\kappa$ ,  $\mu$  and  $m$  [20]. If the parameters  $\mu$  and  $m$  are restricted to be positive integers, then for any arbitrary non-negative real  $\kappa$  the probability density function (PDF) and CDF of  $\gamma$  are given by [23, eq. (4-10)]

$$f_{\mathcal{S}}(x) = \sum_{j=0}^M C_j \underbrace{\frac{x^{m_j-1} e^{-\frac{x}{\Omega_j}}}{\Omega_j^{m_j} (m_j-1)!}}_{f_{\mathcal{K}}(\Omega_j; m_j; x)}, \quad (1)$$

$$F_{\mathcal{S}}(x) = 1 - \sum_{j=0}^M C_j e^{-\frac{x}{\Omega_j}} \sum_{r=0}^{m_j-1} \frac{1}{r!} \left(\frac{x}{\Omega_j}\right)^r \quad (2)$$

where  $M$  and the set of parameters  $\{C_j, m_j, \Omega_j\}_{j=1,\dots,M}$  are expressed in terms of  $\bar{\gamma}$ ,  $\kappa$ ,  $\mu$  and  $m$  according to Table I. In (1)  $f_{\mathcal{K}}(\cdot)$  represents the PDF of a squared Nakagami- $m$  distribution, (i.e. a Gamma distribution).

We must here note that according to Lemma 1, the  $\kappa\text{-}\mu$  shadowed distribution with integer fading parameters  $m$  and  $\mu$  can be expressed as a finite mixture of squared Nakagami- $m$  (or Gamma) distribution. To theoretically obtain the Rician distribution as special case, we need to set  $\mu = 1$  and tend  $m \rightarrow \infty$ . However, in practice, the  $\kappa\text{-}\mu$  shadowed distribution converges rapidly to the Rician distribution, i.e. for  $m \approx 15 - 20$  [23].

*Corollary 2 (Product of Two Squared Nakagami- $m$  RVs):* Let  $Z = W\hat{W}$  be the product of two INID squared Nakagami- $m$  random variables  $W$  and  $\hat{W}$  with means  $\Omega$  and  $\hat{\Omega}$ , where the corresponding shape parameters  $m$  and  $\hat{m}$  are arbitrary positive integer numbers. Then, the corresponding PDF and CDF are given by

$$f_{\Gamma\Gamma}(x) = \frac{2 x^{\frac{m+\hat{m}}{2}-1}}{\Gamma(m)\Gamma(\hat{m})(\Omega\hat{\Omega})^{\frac{m+\hat{m}}{2}}} K_{m-\hat{m}}\left(\sqrt{\frac{4x}{\Omega\hat{\Omega}}}\right), \quad (3)$$

$$F_{\Gamma\Gamma}(x) = 1 - \sum_{k=0}^{m-1} \frac{2}{k! \Gamma(\hat{m})} \left(\frac{x}{\Omega\hat{\Omega}}\right)^{\frac{k+\hat{m}}{2}} K_{\hat{m}-k}\left(\sqrt{\frac{4x}{\Omega\hat{\Omega}}}\right) \quad (4)$$

where  $K_{\nu}$  is the modified Bessel function of the second kind, and  $\Gamma(\cdot)$  is the Gamma function.

*Proof:* The PDF follows from the corresponding expression given in [24] after performing a simple random variable transformation of the type  $Y = X^2$ . The CDF follows from [11, eq. 8] by specializing the parameter  $a = 1$ . ■

The distribution described in Corollary 2 is essentially a Gamma-Gamma ( $\Gamma\Gamma$ ) distribution, up to a trivial re-scaling by  $\Omega$ . For the sake of notation simplicity, in this work we will refer to this distribution as a  $\Gamma\Gamma$  distribution.

### B. Main results

By means of the previous results and considerations, we will now characterize the distribution of the product of two INID  $\kappa\text{-}\mu$  shadowed fading variables with integer fading parameters.

*Proposition 3 (The  $\mathcal{P}$ -distribution as a finite mixture of  $\Gamma\Gamma$  distributions):* Let  $Z$  be the product of two INID squared  $\kappa\text{-}\mu$  shadowed random variables  $X$  and  $\hat{X}$  with means  $\bar{\gamma}$  and  $\tilde{\gamma}$ . The corresponding shape parameters  $\kappa$  and  $\hat{\kappa}$  are arbitrary non-negative real numbers and the remainder shape parameters  $\mu$  and  $m$  for  $X$ , and  $\hat{\mu}$  and  $\hat{m}$  for  $\hat{X}$  are positive integers. Under these conditions,  $Z = X\hat{X}$  is distributed as a  $\Gamma\Gamma$  finite mixture with the following PDF

$$f_Z(z) = \sum_{j=0}^M \sum_{h=0}^{\hat{M}} C_j \hat{C}_h \times \underbrace{\frac{2 z^{\frac{m_j+\hat{m}_h}{2}-1}}{\Gamma(m_j)\Gamma(\hat{m}_h)(\Omega_j\hat{\Omega}_h)^{\frac{m_j+\hat{m}_h}{2}}} K_{m_j-\hat{m}_h}\left(\sqrt{\frac{4z}{\Omega_j\hat{\Omega}_h}}\right)}_{f_{\Gamma\Gamma}(z; \{\Omega_j, m_j\}; \{\hat{\Omega}_h, \hat{m}_h\})} \quad (5)$$

where the parameters  $M$  and  $\{C_j, m_j, \Omega_j\}_{j=1,\dots,M}$  are expressed in terms of  $\bar{\gamma}$ ,  $\kappa$ ,  $\mu$  and  $m$  according to Table I; similarly the parameters  $\hat{M}$  and  $\{\hat{C}_h, \hat{m}_h, \hat{\Omega}_h\}_{h=1,\dots,\hat{M}}$  are also expressed in terms of  $\tilde{\gamma}$ ,  $\hat{\kappa}$ ,  $\hat{\mu}$  and  $\hat{m}$  according to Table I.

*Proof:* See Appendix A. ■

Proposition 3 states that the  $\mathcal{P}$ -distribution can be expressed in closed-form as a finite sum of well-known special functions. Since the  $\mathcal{P}$ -distribution is more general and simpler than the Rician product distribution (which is but a special case for  $\mu = \hat{\mu} = 1$  and sufficiently large  $m$  and  $\hat{m}$ ), we advocate for its use as the reference product channel model in a

TABLE I  
PARAMETER VALUES FOR THE  $\kappa$ - $\mu$  SHADOWED DISTRIBUTION WITH INTEGER  $\mu$  AND  $m$ ,

Case $\mu > m$	Case $\mu \leq m$
$M = \mu$	$M = m - \mu$
$C_i = \begin{cases} 0 & i = 0 \\ (-1)^m \binom{m+i-2}{i-1} \times \left[ \frac{m}{\mu\kappa+m} \right]^m \left[ \frac{\mu\kappa}{\mu\kappa+m} \right]^{-m-i+1} & 0 < i \leq \mu - m \\ (-1)^{i-\mu+m-1} \binom{i-2}{i-\mu+m-1} \times \left[ \frac{m}{\mu\kappa+m} \right]^{i-\mu+m-1} \left[ \frac{\mu\kappa}{\mu\kappa+m} \right]^{-i+1} & \mu - m < i \leq \mu \end{cases}$	$C_i = \binom{m-\mu}{i} \left[ \frac{m}{\mu\kappa+m} \right]^i \left[ \frac{\mu\kappa}{\mu\kappa+m} \right]^{m-\mu-i}$
$m_i = \begin{cases} \mu - m - i + 1, & 0 \leq i \leq \mu - m \\ \mu - i + 1 & \mu - m < i \leq \mu \end{cases}$	$m_i = m - i$
$\Omega_i = \begin{cases} \frac{\gamma}{\mu(1+\kappa)}, & 0 \leq i \leq \mu - m \\ \frac{\mu\kappa+m}{m} \frac{\gamma}{\mu(1+\kappa)} & \mu - m < i \leq \mu \end{cases}$	$\Omega_i = \frac{\mu\kappa+m}{m} \frac{\gamma}{\mu(1+\kappa)}$

communication-theoretic context. This will be later supported by both theoretical and practical evidences in different scenarios of interest.

*Proposition 4 (CDF of the  $\mathcal{P}$  distribution as a finite mixture):* Let  $Z$  be the product of two INID squared  $\kappa$ - $\mu$  shadowed random variables  $X$  and  $\hat{X}$  with means  $\bar{\gamma}$  and  $\hat{\gamma}$ . The corresponding shape parameters  $\kappa$  and  $\hat{\kappa}$  are arbitrary non-negative real numbers and the remainder shape parameters  $\mu$  and  $m$  for  $X$ , and  $\hat{\mu}$  and  $\hat{m}$  for  $\hat{X}$  are positive integers. Under these conditions  $Z = X\hat{X}$  has the following CDF

$$F_Z(z) = \sum_{j=0}^M \sum_{h=0}^{\hat{M}} C_j \hat{C}_h \times \underbrace{\left[ 1 - \sum_{k=0}^{m_j-1} \frac{2}{k! \Gamma(\hat{m}_h)} \left( \frac{z}{\Omega_j \hat{\Omega}_h} \right)^{\frac{k+\hat{m}_h}{2}} \times K_{\hat{m}_h-k} \left( \sqrt{\frac{4z}{\Omega_j \hat{\Omega}_h}} \right) \right]}_{F_{\Gamma\Gamma}(z; \{\Omega_j, m_j\}; \{\hat{\Omega}_h, \hat{m}_h\})} \quad (6)$$

where the parameters  $M$  and  $\{C_j, m_j, \Omega_j\}_{j=1,\dots,M}$ ,  $\hat{M}$  and  $\{\hat{C}_h, \hat{m}_h, \hat{\Omega}_h\}_{h=1,\dots,\hat{M}}$  are those indicated in Theorem 3.

*Proof:* The CDF can be derived from the PDF such as

$$F_Z(z) = \int_0^z f_Z(t) dt. \quad (7)$$

From Proposition 3, we have

$$F_Z(z) = \sum_{j=0}^M \sum_{h=0}^{\hat{M}} C_j \hat{C}_h F_{\Gamma\Gamma} \left( z; \{\Omega_j, m_j\}; \{\hat{\Omega}_h, \hat{m}_h\} \right) \quad (8)$$

where  $F_{\Gamma\Gamma}(\cdot)$  is given by equation (4). ■

Thus, the CDF of the  $\mathcal{P}$ -distribution is also given in a simple closed-form. This expression has important relevance in practice, since the CDF of the product of INID Rician RVs has a very complicated form, which involves a double infinite sum of Meijer  $G$ -functions [19, eq. (23)]. Here, the  $\mathcal{P}$ -distribution function, which includes the Rician product distribution function as a special case, is only given in terms of finite sums of modified Bessel functions of the second

kind. Moreover, this expression also simplifies the CDF of the product built from independent Rayleigh and Rician RVs [19].

We must also note that a similar expression can be given for the moment-generating function, as well as the central moments, which are very useful for certain wireless applications. For the sake of attaining a full statistical characterization of the  $\mathcal{P}$ -distribution, these expressions are provided in the following Propositions.

*Proposition 5 (MGF of the  $\mathcal{P}$  distribution as a finite mixture):* Let  $Z$  be the product of two INID squared  $\kappa$ - $\mu$  shadowed random variables  $X$  and  $\hat{X}$  with means  $\bar{\gamma}$  and  $\hat{\gamma}$ . The corresponding shape parameters  $\kappa$  and  $\hat{\kappa}$  are arbitrary non-negative real numbers and the remainder shape parameters  $\mu$  and  $m$  for  $X$ , and  $\hat{\mu}$  and  $\hat{m}$  for  $\hat{X}$  are positive integers. Under these conditions  $Z = X\hat{X}$  has the following MGF

$$\mathcal{M}_Z(s) = \sum_{j=0}^M \sum_{h=0}^{\hat{M}} C_j \hat{C}_h \frac{e^{-\frac{1}{2s\Omega_j\hat{\Omega}_h}}}{\left( -s\Omega_j\hat{\Omega}_h \right)^{\frac{m_j+\hat{m}_h-1}{2}}} \times \mathcal{W}_{-\frac{m_j+\hat{m}_h-1}{2}, \frac{m_j-\hat{m}_h}{2}} \left( -\frac{1}{s\Omega_j\hat{\Omega}_h} \right) \quad (9)$$

where  $\mathcal{W}_{a,b}(\cdot)$  denotes the Whittaker function [25, eq. 9.220.4], which can be expressed in terms of the Tricomi hypergeometric function.

*Proof:* From (3) the MGF of the  $\Gamma\Gamma$  random variable can be expressed as

$$\mathcal{M}_{\Gamma\Gamma}(s) = \frac{2}{\left( \Omega\hat{\Omega} \right)^{\frac{m+\hat{m}}{2}}} \times \Gamma(m)\Gamma(\hat{m}) \int_0^\infty x^{\frac{m+\hat{m}}{2}-1} e^{sx} K_{m-\hat{m}} \left( \sqrt{\frac{4x}{\Omega\hat{\Omega}}} \right) dx. \quad (10)$$

Applying [26, eq. 4.17.37] to (10) and considering Theorem 3 completes the proof. ■

*Proposition 6 (Central moments of the  $\mathcal{P}$ -distribution):* Let  $Z$  be the product of two INID squared  $\kappa$ - $\mu$  shadowed random variables  $X$  and  $\hat{X}$  with means  $\bar{\gamma}$  and  $\hat{\gamma}$ . The corresponding shape parameters  $\kappa$  and  $\hat{\kappa}$  are arbitrary non-negative real

numbers and the remainder shape parameters  $\mu$  and  $m$  for  $X$ , and  $\hat{\mu}$  and  $\hat{m}$  for  $\hat{X}$  are positive integers. Under these conditions,  $Z = X\hat{X}$  has the following central moments

$$E[Z^n] = \sum_{j=0}^M \sum_{h=0}^{\hat{M}} C_j \hat{C}_h \frac{(\Omega_j \hat{\Omega}_h)^n}{\Gamma(m_j) \Gamma(\hat{m}_h)} \times (m_j + n - 1)! (\hat{m}_h + n - 1)! \quad (11)$$

*Proof:* See Appendix ??.

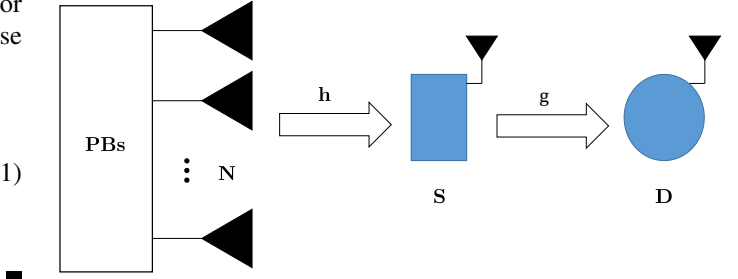


Fig. 1. System Model for Wireless Powered Communications.

### III. WIRELESS POWERED COMMUNICATIONS

Wireless communication systems have classically been analyzed under the assumption of ideal power availability for transmitting and receiving signals. However, in many scenarios such as wireless sensor networks or RFID systems, the autonomy (and therefore performance) of mobile devices is limited in practice by the finite capacity of their batteries. Even though batteries can be replaced or recharged, the cost in time, money and flexibility is not acceptable in many situations, and therefore other alternatives relying on ambient energy harvesting are considered. Besides solar or wind, the use of RF energy is recently being considered as an alternative for the operation of wirelessly powered devices. Specifically, Wireless Powered Communications (WPC) are a promising solution to overcome such limitations, by using dedicated power beacons (PBs) that wirelessly convey the required energy to the network elements to enable their operation [27].

#### A. System Model

Let us consider the scenario in Fig. 1 [10, 11], on which a source S communicates with a destination D with the help of dedicated PBs that wirelessly transfer energy to S. Both S and D are equipped with a single antenna, while PBs are equipped with  $N$  antennas. The system operation follows a *harvest-then-transmit*-like policy for every time transmission interval  $T$ , as follows: during the first  $\tau T$  seconds (with  $0 < \tau < 1$ ), the source S harvests energy from the PBs. During the energy harvesting phase, the received signal at S can be expressed as

$$y_S = \sqrt{\frac{P}{d_1^\alpha}} \mathbf{h} \mathbf{x}_S + n_S \quad (12)$$

where  $P$  is the transmit power at the PB,  $d_1$  denotes the distance between PB and S,  $\alpha$  is the path loss exponent,  $\mathbf{h}$  and  $\mathbf{x}_S$  are  $N$  elements vectors denoting the channel response and the transmitted symbols, respectively, and  $n_S$  is the additive white Gaussian noise (AWGN) with  $E\{n_S n_S^*\} = 0$ . The elements of  $\mathbf{h} = [h_i]$  ( $i = 1 \dots N$ ) are assumed to be independent and identically distributed (i.i.d.) with unitary variance. Assuming  $\mathbf{x}_S$  is formed with optimal beamforming, the total energy received at the end of the first phase is

$$E_n = \frac{\eta \|\mathbf{h}\|^2 P \tau T}{d_1^\alpha} \quad (13)$$

where  $0 < \eta < 1$  is the energy conversion efficiency.

In the second phase, S transmits information to D using the energy harvested in the first phase during  $(1 - \tau)T$  seconds. Hence, the received signal  $y_D$  at D is given by

$$y_D = \sqrt{\frac{E_n}{(1 - \tau)T d_2^\alpha}} g s_0 + n_d \quad (14)$$

where  $d_2$  denotes the distance between S and D,  $g$  is the channel response following an arbitrary fading distribution with unit variance,  $s_0$  is the information symbol with unit energy, and  $n_d$  is AWGN with variance  $N_0$ . Therefore, the instantaneous end-to-end signal to noise ratio (SNR) can be computed as

$$\gamma = \frac{\tau \eta \|\mathbf{h}\|^2 |g|^2 P}{(1 - \tau) d_1^\alpha d_2^\alpha N_0}. \quad (15)$$

#### B. Performance analysis

Direct inspection of (15) reveals that the distribution of  $\gamma$  is that of the product of  $\|\mathbf{h}\|^2$  and  $|g|^2$ , which is ultimately related to the distribution of the product of the underlying fading channels between PBs and S, and between S and D. As argued in [10], the link between PBs and S is inherently LOS because of the relatively short distance between both agents. However, the consideration of the Rician distribution to model the small-scale fading in the PBs-S link is associated to a larger mathematical complexity. For this reason, the Rician distribution was approximated by the Nakagami- $m$  distribution with integer  $m$  for the sake of tractability in [10], by setting  $m = \lfloor (1 + K)^2 / (1 + 2K) \rfloor$ , where  $\lfloor p \rfloor$  denotes the nearest integer to  $p$ . The S-D link will be NLOS or LOS depending on the specific set-up: both situations were addressed in [10] and [11] by resorting to Rayleigh and Nakagami- $m$  fading, respectively.

In the most general situation, both the PBs-S and the S-D links can be LOS, and therefore the product channel associated to LOS scenarios is the natural choice for characterizing the behavior of the end-to-end SNR. We here propose the use of the  $\mathcal{P}$ -distribution introduced in Section II for this application, as a workaround to characterize the distribution of  $\gamma$  when the Rician distribution is considered. Because  $\|\mathbf{h}\|^2$  can be expressed as the sum of  $N$  squared Rician random variables (i.e. a  $\kappa$ - $\mu$  distribution with  $\kappa = K$  and  $\mu = N$ ), and assuming  $|g|^2$  to be Rician distributed, the distribution of  $\gamma$  is that of the product of  $\kappa$ - $\mu$  and Rician random variables. Thus, it arises as a special case of the  $\mathcal{P}$ -distribution. Compared to the

approximation in [10], our approach has a number of benefits which can be summarized as follows:

- The Rician shadowed distribution ( $\kappa\text{-}\mu$  shadowed distribution with  $\mu = 1$ ) and the Rician distribution have a diversity order equal to one, as opposed to the Nakagami- $m$  distribution, for which the diversity order is  $m$ . Thus, approximating the Rician distribution by the Rician shadowed distribution does not affect the diversity order. As we will later see, this has an impact in the asymptotic performance for low SNR values.
- The Rician shadowed distribution explicitly uses the same  $K$  parameter as the Rician distribution. Therefore, there is no need to use rounding as in the Nakagami- $m$  approximation when setting  $m = \lfloor (1+K)^2/(1+2K) \rfloor$ .
- In practice, LOS channels will not be purely Rician because of the inherent fluctuation of the LOS component [28]. In fact, the  $\kappa\text{-}\mu$  shadowed fading model always provides a better fit to real measurements than the Rician fading model alone, just because the latter is a special case of the former. Thus, the  $\mathcal{P}$ -distribution is not only simpler and more general than the Rician product distribution, but also closer to the real behavior of the fading channel.

With all the above considerations, the performance of WPC systems in LOS scenarios can be easily evaluated when considering the  $\mathcal{P}$ -distribution. Assuming that S transmits at a constant rate  $R_c$ , which may be subjected to outage due to fading, the average throughput can be evaluated as

$$R_{DC} = (1 - P_{\text{out}}) R_c (1 - \tau) \quad (16)$$

where  $P_{\text{out}} = \Pr\{\gamma < \gamma_{\text{th}}\}$  is the outage probability. As previously stated, the distribution of the product  $\|\mathbf{h}\|^2 \cdot |g|^2$  can be modeled as a product of two independent squared  $\kappa\text{-}\mu$  shadowed variables with a proper choice of parameters. Thus, the outage probability can be obtained from (6) as

$$P_{\text{out}} = F_{\gamma} \left( \frac{(1 - \tau) d_1^{\alpha} d_2^{\alpha} N_0}{\tau \eta P} \gamma_{\text{th}} \right). \quad (17)$$

### C. Numerical Results

We now use the results in the previous subsection for evaluating to what extent the Rician product channel can be approximated by a Nakagami- $m$  product channel, in the context of WPC scenarios. The following set of parameters is considered, in coherence with those used in [10]:  $R_c = 1$  bps/Hz, which implies an outage SNR threshold given by  $\gamma_{\text{th}} = 2^{R_c} - 1 = 1$ , the harvesting time is set to 50% of the interval  $T$ , the energy conversion efficiency is set to  $\eta = 0.4$ , path loss exponent is set to  $\alpha = 2.5$ , and distances are set to be  $d_1 = 8$  m and  $d_2 = 15$  m, respectively.

In Fig. 2, the throughput obtained from (16) is evaluated as a function of the average SNR, for different numbers of antennas at the PBs. Because of the beamforming strategy used by the PBs, the distribution of  $\|\mathbf{h}\|^2$  is that of a squared  $\kappa\text{-}\mu$  random variable. We first assume that the channel between the source S and the destination D is NLOS as in [10], so it can be safely modeled by a Rayleigh fading channel. Thus, we

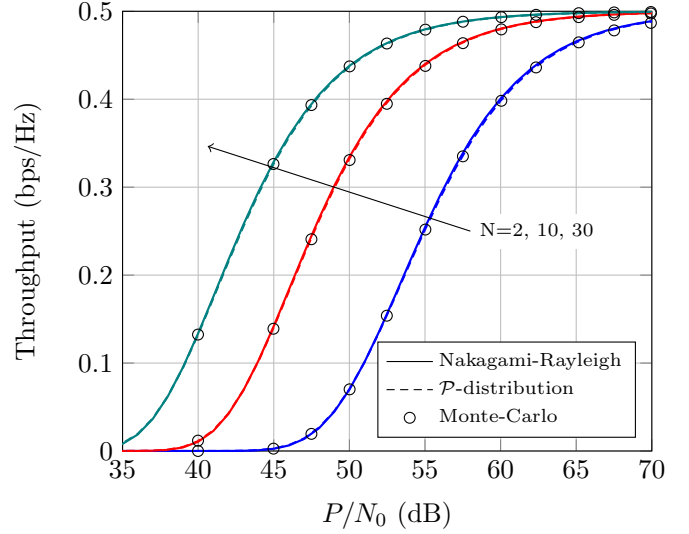


Fig. 2. Average Throughput  $R_{DC}$  vs average SNR, for different values of  $N$ . LOSxNLOS scenario. MC simulations correspond to the Rician-Rayleigh case.

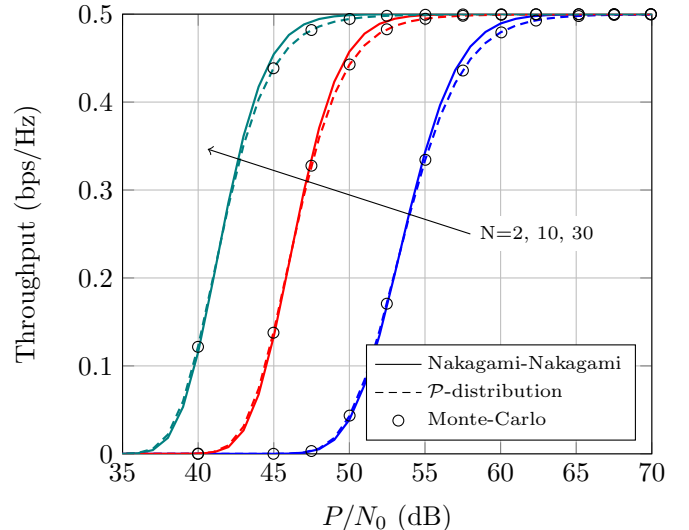


Fig. 3. Average Throughput  $R_{DC}$  vs average SNR, for different values of  $N$ . LOSxLOS scenario. MC simulations correspond to the Rician-Rician case.

here compare two alternatives for evaluating (16): the first one is approximating  $\|\mathbf{h}\|^2$  by a squared Nakagami- $m$  (gamma) distribution with  $m = \lfloor (1+K)^2/(1+2K) \rfloor \cdot N$  as in [10], and then using the statistics of a Nakagami-Rayleigh product channel; the second one is using the  $\mathcal{P}$ -distribution with  $\kappa = K$ ,  $\mu = N$ ,  $\hat{\kappa} = 0$ ,  $\hat{\mu} = 1$ , and sufficiently large  $m$  and  $\hat{m}$  (i.e.  $m = \hat{m} = 20$ ). We consider  $K = 3 + \sqrt{12}$  for the Rician  $K$  factor parameter, so that the rounding error inherent to the approximation in [10] is zero. We observe that both approaches yield very similar results for the set of parameters here considered. Thus, the approximation can be safely used when considering a product channel built from a LOS and a NLOS individual channels, for the evaluation of (16).

However, things change when *both* channels are considered to be LOS. In Fig. 3, the S-D link is also assumed to be

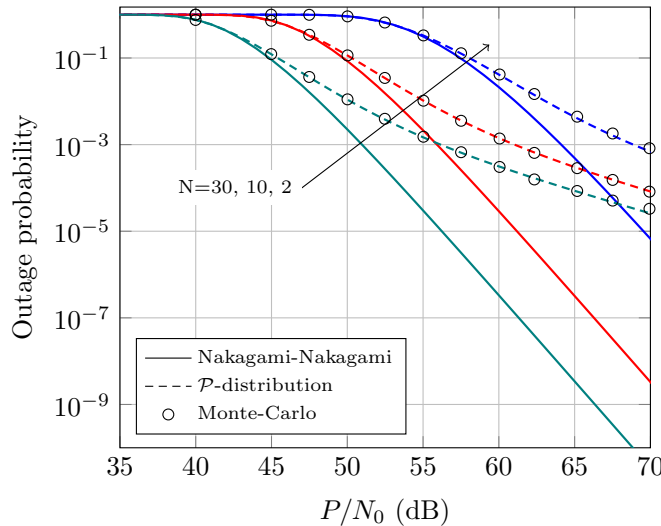


Fig. 4. Outage probability vs average SNR, for different values of  $N$ . LOS $\times$ LOS scenario. MC simulations correspond to the Rician-Rician case.

LOS with equal  $K$  parameter as in Fig. 2. We now see a noticeable difference between the approximation in [10] and the exact result using the  $\mathcal{P}$ -distribution with  $\kappa = \hat{\kappa} = K$ ,  $\mu = N$ ,  $\hat{\mu} = 1$  and  $m = \hat{m} = 20$ , which perfectly matches the Monte-Carlo simulations run for the Rician product case. This becomes even more evident when analyzing the tail behavior of the outage probability in Fig. 4, where the different diversity orders of the Nakagami- $m$  distribution and the Rician distribution can be observed. Thus, it is not recommended to use the Nakagami- $m$  product channel as an approximation of the Rician product channel, due to the lack of accuracy when modeling LOSxLOS channels, especially in the high-SNR regime.

#### IV. BACKSCATTER COMMUNICATIONS

Backscatter radio systems base their operation in the ability to detect power from specular reflections, and can be traced back to the late 40's [29]. These systems have been widely used in tropospheric communications or radar, evolving to other applications such as RF identification (RFID) [19] and RF modulated backscatter (RFMB), also known as modulated radar cross section or sigma modulation [13].

Here, we revisit the results provided in [13] [19] and [30], where backscatter communications are modeled with Rician product channels. We will see that employing the  $\mathcal{P}$ -distribution simplifies the theoretical analysis, while also improving the accuracy when fitting to real channel measurements.

##### A. Bistatic RFID systems

Since the beginning of the 21st century, RFID systems have gained substantial popularity. The possibility of using passive receivers (or tags) that can operate without requiring additional batteries has attracted extreme hype for many applications where power constraints are very strict, including indoor localization and industrial automation [31]. The principle of

operation is simple: Passive tags contain electronically stored information. When excited by an incident signal, they scatter a portion of this signal, which is transmitted back to the tag reader.

When compared to conventional RF communication systems, RFID systems involve two different communication links: the power-up (forward) link and the backscatter (reverse) link, which are inherently LOS [19]. This produces a received signal whose fluctuation typically exhibits a more severe fading than classical fadings, which is usually modeled by a product of two Rician processes [19].

We distinguish two types of RFID communications: monostatic and bistatic. While monostatic RFID communications use the same antennas for transmitting and receiving purposes, bistatic RFID systems require different antennas, as shown in Fig. 5. By an appropriate positioning of the two readers, bistatic systems can achieve a larger reading range [19], as well as they have better system performance in general since they have dedicated antennas to send and receive signals. In turn, monostatic RFID solutions are cheaper since they are comprised of a lower number of antennas.

Despite the great performance of bistatic solutions, the analysis of resulting communication channels in a tractable form is still an open problem of the literature, since, in the simplest case possible, it requires the characterization of the product of two INID Rician RVs, whose PDF involves double infinite sums of special functions [32, eq. (6.66)]. We will here show that using the novel  $\mathcal{P}$ -distribution greatly simplify the challenge.

Let us consider the system model for bistatic RFID communications in Fig. 5, where the reader 1 sends an RF signal which is scattered by the passive tag and sent back to reader 2. The signal power  $P_R$  received is proportional to [19, eq. (12)]

$$P_R = \bar{P}_R |h_f|^2 |h_b|^2 \quad (18)$$

where  $\bar{P}_R$  is average power received by reader 2, while  $h_f$  and  $h_b$  are the normalized fading coefficients of each link. From (18), we observe that the resulting channel is equivalent to a cascade of two channels, due to the forward and reverse links. Since both links are inherently LOS, the power channel gains  $|h_f|^2$  and  $|h_b|^2$  have been usually modeled by square Rician variables. Here, we will characterize the distribution of  $P_R$  by using the  $\mathcal{P}$ -distribution.

We are interested on the detection probability as a performance metric, which is defined as [19, eq. (17)]

$$\mathcal{D} \triangleq \Pr\{P_R \geq S_R\} \quad (19)$$

$$= 1 - \text{Prob}(P_R < S_R) \quad (20)$$

where  $S_R$  is the sensitivity of the reader antenna 2. Define  $P_{\text{th}} = S_R / \bar{P}_R$ , then

$$\mathcal{D} = 1 - F_Z(P_{\text{th}}) \quad (21)$$

where  $F_Z(z)$  is the CDF of the product model. When using the  $\mathcal{P}$ -distribution, this CDF only involves finite sums of modified Bessel functions of the second kind (see Proposition 4). When using the classical Rician product CDF, we have a double infinite sum of Meijer  $G$ -functions, which makes harder the evaluation of the detection probability.

Fig 6 presents the detection probability of the bistatic RFID system of Fig. 5. For the sake of simplicity, we have assumed that, in each scenario, both forward and reverse links have the same statistical characterization, and the sensitivity of receiver 2 is  $S_R = -75$  dBm. We have studied four Rician-Rician scenarios, whose Rician  $K$ -factors are  $K = 0$  (Rayleigh),  $K = 3.5$ ,  $K = 8$  and  $K = 13$ . As discussed in [23], one possibility is approximating the Rician distribution by a Rician shadowed distribution with sufficiently large  $m$ .

We here propose a different alternative, which can be of use when we are interested on obtaining a similar tail behavior for both distributions, *both* in terms of the diversity orders and the diversity gains. For each Rician-Rician scenario, we approximate Rician random variables through  $\kappa$ - $\mu$  shadowed random variables with  $\mu = 1$ , and then find the values of  $m$  and  $\kappa$  that provide the best fit to the CDF tail for a finite  $m$ .

We see a perfect agreement between the curves derived with the Rician product distribution and those derived with the  $\mathcal{P}$ -distribution, which are double-checked through Monte-Carlo simulations. Therefore, when appropriately choosing the values of the  $\mathcal{P}$ -distribution parameters, we can reproduce any Rician-Rician scenario. Consider the Rician-Rician scenario with  $K = 13$  of Fig. 6. We observe that we can employ the  $\mathcal{P}$ -distribution with  $\kappa = 20$  and  $m = 20$  to reproduce such scenario. For obtaining an equivalent tail behavior for the Rician-Rician scenario with  $K = 8$ , we need to set  $\kappa = 10$  and  $m = 20$  for the  $\mathcal{P}$ -distribution parameters. As for the Rician-Rician scenario with  $K = 3.5$ , this can be approximated by the  $\mathcal{P}$ -distribution with  $\kappa = 10$  and  $m = 4$ . We see that modeling LOSxLOS scenarios for any value of the Rician  $K$ -factor can be performed with the  $\mathcal{P}$ -distribution by a proper tuning of  $\kappa$  and  $m$ , which illustrates the flexibility of the  $\mathcal{P}$ -distribution. For the Rician-Rician scenario on which  $K = 0$  (i.e. Rayleigh), the value of the  $\mathcal{P}$ -distribution parameter  $m$  has been set to the unit value since it does not modify the shape of the distribution.

Moreover, we must highlight that  $m \leq 20$  for all the scenarios considered. This has important relevance in practice since we can analyze LOS product models by using the  $\mathcal{P}$ -distribution approximation with finite  $m$ , instead of using the classical Rician product distribution, which does not have a tractable characterization. To evaluate important performance measures, we will only require a finite sum of few special functions, e.g. modified Bessel functions for the CDF.

### B. RF Modulated Backscatter Systems

RFMB is an RF technique useful for short range, typically 1–15m, and low data rate applications, i.e. up to tens of kbps [31]. Its operation principle can be illustrated by Fig. 7. The RF carrier is modulated at the low-power modulator, which gives a reflected signal, also known as backscattered signal. Therefore, similarly as the analysis of bistatic RFID link, the exact characterization of such resulting channel involves the product of two LOS processes, which we here model with the  $\mathcal{P}$ -distribution.

Fig. 8 shows a comparison between the CDF measurement performed in [13], the Rician-Rician fitting provided in [13]

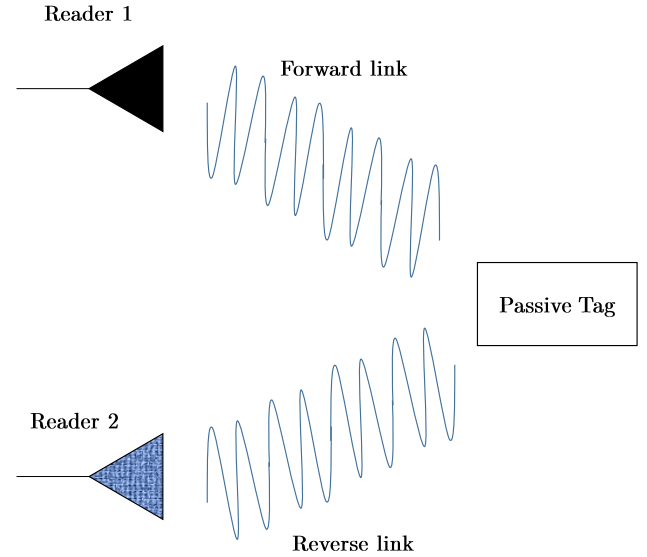


Fig. 5. System Model for Bistatic RFID.

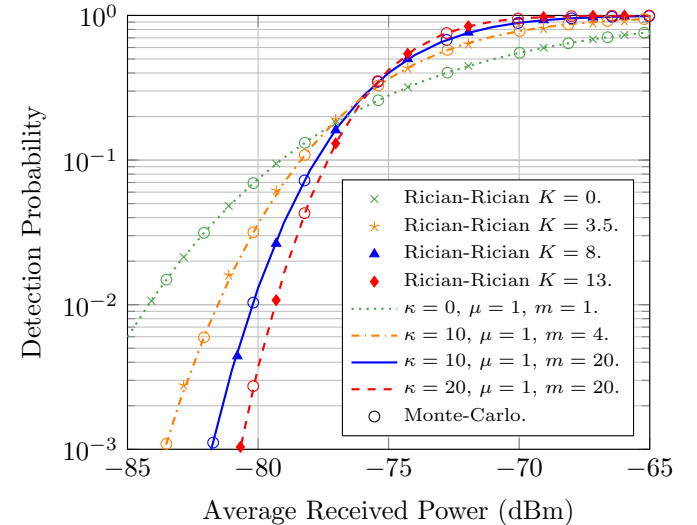


Fig. 6. Detection probability for bistatic RFID systems.

and the corresponding theoretical curve obtained with the  $\mathcal{P}$ -distribution. Like in [13], we have assumed that both forward and reverse links have the same statistics. In addition to simplifying the characterization of such product LOS channel, we must note that there is a outstanding agreement between measurements and the theoretical analysis with the  $\mathcal{P}$ -distribution, even for a very low value of the shadowing parameter ( $m = 4$ ). Again, this reflects the usefulness of the  $\mathcal{P}$ -distribution. Although the Rician model is theoretically obtained by tending  $m$  to infinity, in practice we only need small values of this parameter, as argued in [23]. By only evaluating 64 (3 nested finite sums of 4 terms) modified Bessel of second kind, which is immediate, we see a slightly better fitting with our  $\mathcal{P}$ -distribution than the corresponding one with the Rician product model in [13]. To evaluate the improvement, we define an error factor  $\epsilon$  based on a modified

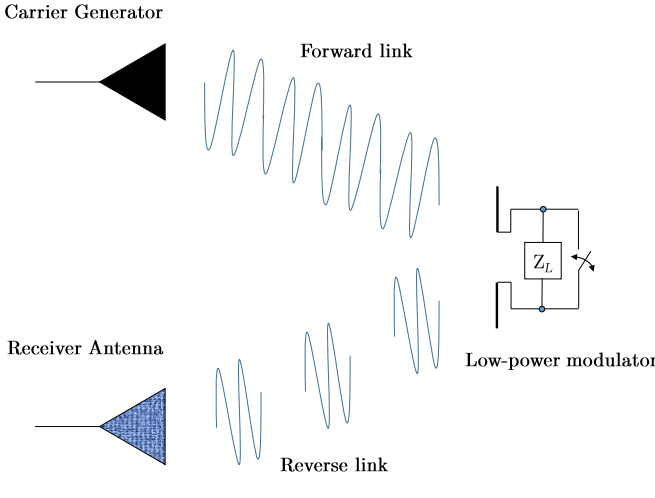


Fig. 7. System Model for RFMB.

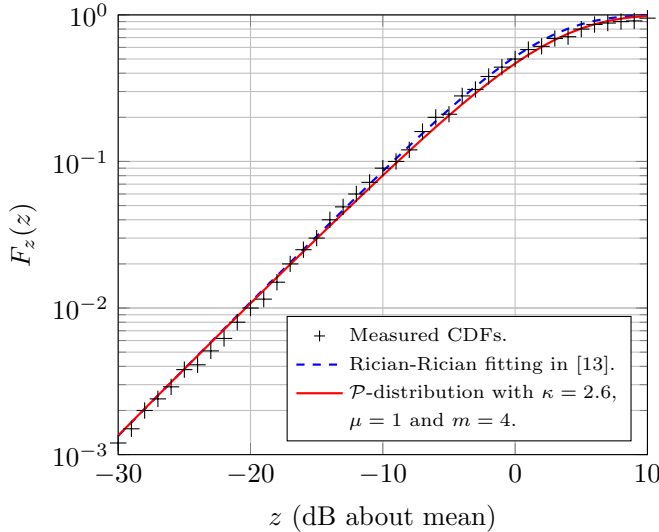


Fig. 8. Empirical vs theoretical CDFs of RF modulated backscatter system.

version of the Kolmogorov-Smirnov (KS) statistic, i.e.

$$\epsilon \triangleq \max_x |\log_{10} \tilde{F}_Z(x) - \log_{10} F_Z(x)| \quad (22)$$

where  $\tilde{F}_Z(x)$  and  $F_Z(x)$  are the empirical and theoretical CDFs, respectively. Note that, with the above definition, a value of  $\epsilon = 1$  corresponds to a difference of one order of magnitude between empirical and theoretical CDFs. With such KS statistic, the error factor value for the fitting proposed in [13] with the Rician product model is  $\epsilon^{\text{Rician}} = 0.0882$ , while the corresponding one with the  $\mathcal{P}$ -distribution is  $\epsilon^{\mathcal{P}} = 0.0793$ .

Therefore, the advantages of using the  $\mathcal{P}$ -distribution instead of the classical Rician product distribution are evident. The analysis of systems that involve two different communication LOS links is simplified, which facilitates the computation of relevant performance measures, and, at the same time, using the  $\mathcal{P}$ -distribution does not compromise the accuracy when fitting measurements, but it rather improves it.

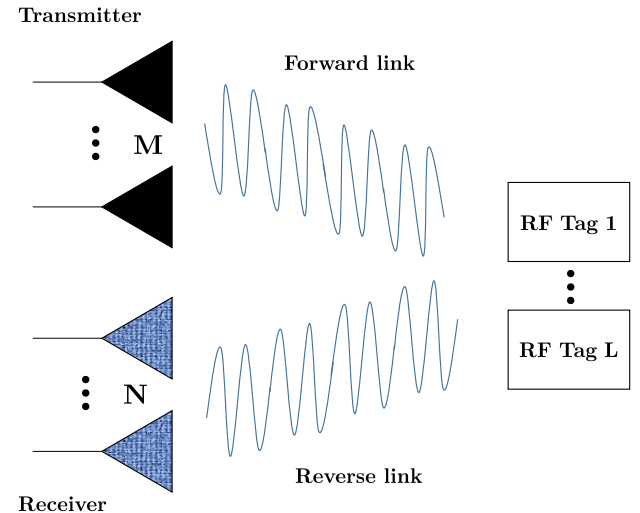


Fig. 9. System Model for Dyadic Backscatter Channel.

### C. Dyadic Backscatter Systems

When compared to previous backscatter systems, the so-called dyadic ones employ multiple antennas in both forward and reverse links to reduce the fading severity. The most general set-up comprises an  $M$ -antenna reader transmitter,  $L$  RF tags and an  $N$ -antenna reader receiver, and the equivalent channel model is usually referred to as the dyadic backscatter channel (DBC) [14, 30]. The use of multiple RF tags effectively reduces the severity of fading in NLOS scenarios, as the equivalent channel can be seen as a product channel built from the sum of products of Rayleigh channels, thus taking advantage of the *pinhole diversity* as  $L$  increases [14, 30].

The theoretical formulation of the DBC is based on the Rayleigh product distribution, mainly due to tractability reasons. However, in these scenarios the forward and reverse links are inherently LOS, as argued before. Thus, a better fit to field measurements is exhibited when considering a DBC built from the product of Rician fading channels. We will show again how the  $\mathcal{P}$ -distribution is well-suited for this situation.

Let us consider the system model in Fig. 7. The transmitter unit is equipped with  $M$  antennas and the receiver unit has  $N$  antennas. The resulting channel is the cascade of two channels, due to the forward and backscatter links. We denote it  $M \times L \times N$  channel. The signal amplitude  $y_j$  received at the  $j$ -th antenna is proportional to the sum of  $M$  products of the form

$$y_j \propto (h_1 + h_2 + \dots + h_M) g_j \quad (23)$$

where  $h_i$  and  $g_j$  are the forward and backscatter channel responses from antennas  $i$  and  $j$ , modeled as complex Gaussian circularly symmetric random variables with variances  $\sigma_f^2$  and  $\sigma_b^2$ , respectively. Assuming independency among the  $h_i$  elements, the sum  $(h_1 + h_2 + \dots + h_M)$  is also a complex Gaussian variable but of variance  $M\sigma_f^2$ . The effect of using  $M$  antennas translates into a scaling of the overall power received at the  $j$ -th antenna port by  $M$ . Thus,  $y_j$  is proportional to a product of two complex Gaussian variables. In a general LOS

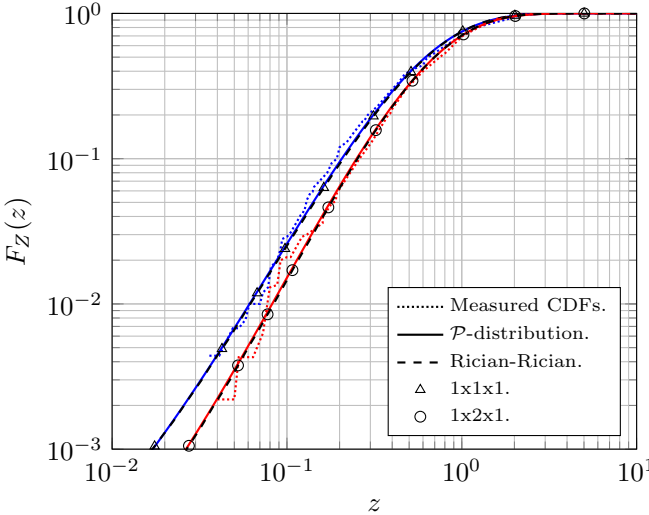


Fig. 10. Empirical vs theoretical CDFs at RX1 in [30]. Parameter values are  $(\kappa_{1 \times 1 \times 1} = 12, \mu_{1 \times 1 \times 1} = 1, m_{1 \times 1 \times 1} = 9)$  and  $(\kappa_{1 \times 2 \times 1} = 10, \mu_{1 \times 2 \times 1} = 1, m_{1 \times 2 \times 1} = 20)$  for the  $\mathcal{P}$ -distribution, and  $K_{1 \times 1 \times 1} = 7$  and  $K_{1 \times 2 \times 1} = 8$  for the Rician product distribution.

TABLE II  
KS ERROR FACTOR  $\epsilon$

Configuration	RX1		RX2	
	$\epsilon_{\text{Rician}}$	$\epsilon^{\mathcal{P}}$	$\epsilon_{\text{Rician}}$	$\epsilon^{\mathcal{P}}$
$1 \times 1 \times 1$	0.1135	0.1067	0.3848	0.3542
$1 \times 2 \times 1$	0.2107	0.2086	0.2589	0.2555

scenario, the signal envelope  $|y_j|$  will be the product of two Rician variables. Similarly as in previous sections, we can characterize such product with the  $\mathcal{P}$ -distribution.

Figs. 10 and 11 present the empirical results for DBC provided in [30]. Two different DBCs are considered:  $1 \times 1 \times 1$  and  $1 \times 2 \times 1$ , i.e. we consider single-tag and double tag configurations, with a single antenna at both the transmitter and receiver side. There are two set of measurements, which correspond to different receiver antennas, namely RX1 and RX2, and are plotted in Fig. 10 and Fig. 11, respectively. Further details on the specific measurement set-up can be found in [30].

Figs. 10 and 11 also depict two different fittings with the Rician-Rician and the  $\mathcal{P}$  distributions. We clearly see that the empirical CDFs are well modeled with both LOS product model. To quantify the goodness of each fitting, we have computed the KS error factor defined in (22). Table II presents the values of this error factor for each case. We observe no substantial difference between the fitting provided by the Rician-Rician distribution and the  $\mathcal{P}$ -distribution. Thus, we advocate the  $\mathcal{P}$ -distribution as the reference product channel distribution in a communication-theoretic context, since it always yields a better performance in LOS scenarios than the classical Rician-Rician product model (just because the latter is a special case of the former), while at the same time admitting a simple closed-form statistical characterization.

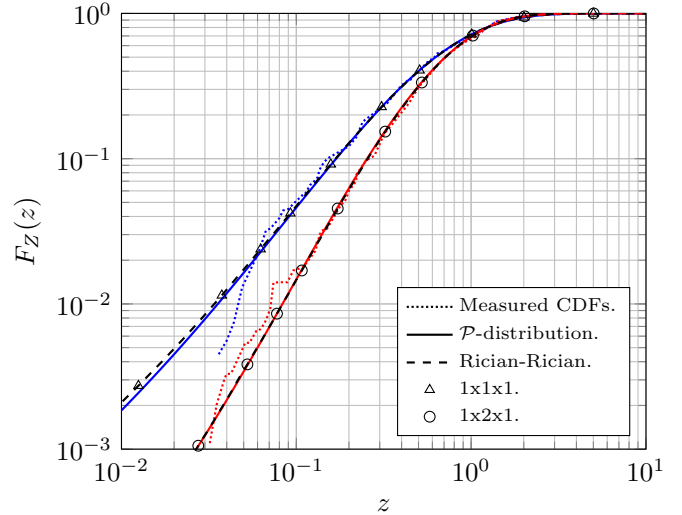


Fig. 11. Empirical vs theoretical CDFs at RX2 in [30]. Parameter values are  $(\kappa_{1 \times 1 \times 1} = 8, \mu_{1 \times 1 \times 1} = 1, m_{1 \times 1 \times 1} = 8)$  and  $(\kappa_{1 \times 2 \times 1} = 11, \mu_{1 \times 2 \times 1} = 1, m_{1 \times 2 \times 1} = 15)$  for the  $\mathcal{P}$ -distribution, and  $K_{1 \times 1 \times 1} = 5$  and  $K_{1 \times 2 \times 1} = 7.9$  for the Rician product distribution.

## V. CONCLUSIONS

We have simplified the study of LOS product fading channels, for which results are generally complicated thus far due to the significant analytical challenge posed by the product of Rician RVs. We have introduced a new model based on the product of two INID  $\kappa$ - $\mu$  shadowed RVs, which has allowed us to characterize LOS product channels models with very simple closed-form expressions. In particular, we have characterized the PDF, CDF and MGF in terms of finite sums of well-known special functions, which can be found in commercial mathematical packages. The usefulness of the results have been exemplified through the analysis of WPC and backscatter communication systems. Specifically, we have observed that previous channel approximations based on the Nakagami- $m$  distribution failed to provide good accuracy for such non-ergodic measures in LOSxLOS scenarios. Moreover, in addition to simplifying previous exact theoretical results for LOSxLOS and LOSxNLOS product channels, our model has better flexibility when fitting experimental results, which makes the  $\mathcal{P}$ -distribution the most suitable choice to model LOS product channels.

## APPENDIX A PROOF OF PROPOSITION 3

The MGF of  $Z$  can be computed as

$$\mathcal{M}_Z(s) \triangleq E \left[ e^{s\hat{X}s} \right] = \int_0^\infty E \left[ e^{s\hat{X}s} \mid X = x \right] f_X(x) dx = \int_0^\infty f_X(x) \mathcal{M}_{\hat{X}}(sx) dx. \quad (24)$$

Now, according to Corollary 1 the MGF of  $\hat{X}$  in (24) can be expressed in terms of the squared Nakagami- $m$  MGF  $\mathcal{M}_{\mathcal{K}}$  as follows

$$\mathcal{M}_{\hat{X}}(sx) = \sum_{h=0}^{\hat{M}} \hat{C}_h \mathcal{M}_{\mathcal{K}} \left( \hat{\Omega}_h; \hat{m}_h; sx \right). \quad (25)$$

Using (1) and (25) in (24) and expanding the integrand yields

$$\mathcal{M}_Z(s) = \sum_{j=0}^M \sum_{h=0}^{\hat{M}} C_j \hat{C}_h \times \underbrace{\int_0^\infty f_{\mathcal{K}}(\Omega_j; m_j; x) \mathcal{M}_{\mathcal{K}}(\hat{\Omega}_h; \hat{m}_h; sx) dx}_{\mathcal{M}_{\Gamma\Gamma}(s; \{\Omega_j, m_j\}; \{\hat{\Omega}_h, \hat{m}_h\})} \quad (26)$$

where  $\mathcal{M}_{\Gamma\Gamma}(s; \{\Omega_j, m_j\}; \{\hat{\Omega}_h, \hat{m}_h\})$  is the MGF of the  $\Gamma\Gamma$ . Thus, applying the inverse Laplace Transform in (26) and considering (3) completes the proof.

## APPENDIX B PROOF OF PROPOSITION 6

The central moments of the product of two INID squared Nakagami- $m$  random variables are given by

$$E[Z_{\Gamma\Gamma}^n] = \frac{2}{(\Omega\hat{\Omega})^{\frac{m+\hat{m}}{2}} \Gamma(m) \Gamma(\hat{m})} \int_0^\infty x^{\frac{2n+m+\hat{m}}{2}-1} K_{m-\hat{m}}\left(\sqrt{\frac{4x}{\Omega\hat{\Omega}}}\right) dx. \quad (27)$$

In order to solve the integral in (27), let us consider the following function

$$\Lambda(t) \triangleq \int t^{2q+p-1} K_p(t) dt, \quad (28)$$

where  $q \geq 1$  and  $p \geq 0$  are integer numbers. Taking into account that [33, eq. 11.3.27]

$$\frac{d}{dz} z^\nu K_\nu(z) = -z^\nu K_{\nu-1}(z), \quad (\nu > 0) \quad (29)$$

and iteratively integrating by parts in (28), the following formula is obtained for  $\Lambda(t)$

$$\Lambda(t) = - \sum_{r=1}^m 2^{r-1} \frac{(q-1)!}{(q-r)!} t^{2(q-r)} t^{p+r} K_{p+r}(t). \quad (30)$$

Using [33, eq. 9.7.2], it follows that  $\Lambda(\infty) = 0$ . On the other hand, after considering [33, eq. 9.6.8] and [33, eq. 9.6.9], the value for  $\Lambda(t)$  in  $t = 0$  is given by

$$\Lambda(0) = -2^{q-1} (q-1)! (p+q-1)! 2^{p+q-1}. \quad (31)$$

Since  $K_\nu = K_{-\nu}$ , without loss of generality we can consider  $m \geq \hat{m}$  in the integral of (27) and we can work with  $K_{|\nu|}$  instead of  $K_\nu$ . Thus, after the change of variable  $\frac{4}{\Omega\hat{\Omega}}x = t^2$ , setting  $p = |m - \hat{m}|$  and  $q = \hat{m}$ , we can obtain

$$E[Z_{\Gamma\Gamma}^n] = \frac{(\Omega\hat{\Omega})^n}{\Gamma(m) \Gamma(\hat{m})} (n+m-1)! (n+\hat{m}-1)! \quad (32)$$

After considering Proposition 3 the proof is complete.

## REFERENCES

- [1] M. D. Springer and W. E. Thompson, "Bayesian confidence limits for the reliability of cascade exponential subsystems," *IEEE Transactions on Reliability*, vol. R-16, no. 2, pp. 86-89, Sept 1967.
- [2] S. Nadarajah and S. Kotz, "Exact distribution of the peak runoff," *Journal of Hydrology*, vol. 338, no. 3-4, pp. 325 - 327, 2007.
- [3] Y. Sumitomo and S.-H. H. Tye, "Stringy mechanism for a small cosmological constant," *Journal of Cosmology and Astroparticle Physics*, vol. 2012, no. 08, p. 032, 2012.
- [4] J. Salo, H. M. El-Sallabi, and P. Vainikainen, "The distribution of the product of independent Rayleigh random variables," *IEEE Trans. Antennas Propag.*, vol. 54, no. 2, pp. 639-643, Feb 2006.
- [5] G. K. Karagiannidis, N. C. Sagias, and P. T. Mathiopoulos, "N\*Nakagami: a novel stochastic model for cascaded fading channels," *IEEE Trans. Commun.*, vol. 55, no. 8, pp. 1453-1458, Aug 2007.
- [6] D. Chizhik, G. J. Foschini, M. J. Gans, and R. A. Valenzuela, "Key-holes, correlations, and capacities of multielement transmit and receive antennas," *IEEE Trans. Wireless Commun.*, vol. 1, no. 2, pp. 361-368, Apr 2002.
- [7] V. Erceg, S. J. Fortune, J. Ling, A. J. Rustako, and R. A. Valenzuela, "Comparisons of a computer-based propagation prediction tool with experimental data collected in urban microcellular environments," *IEEE J. Sel. Areas Commun.*, vol. 15, no. 4, pp. 677-684, May 1997.
- [8] S. K. Yoo, S. L. Cotton, P. C. Sofotasios, and S. Freear, "Shadowed fading in indoor off-body communication channels: a statistical characterization using the  $\kappa$ - $\mu$ /gamma composite fading model," *IEEE Trans. Wireless Commun.*, vol. 15, no. 8, pp. 5231-5244, Aug 2016.
- [9] M. Al-Habash, L. C. Andrews, and R. L. Phillips, "Mathematical model for the irradiance probability density function of a laser beam propagating through turbulent media," *Optical Engineering*, vol. 40, no. 8, pp. 1554-1562, 2001.
- [10] C. Zhong, X. Chen, Z. Zhang, and G. K. Karagiannidis, "Wireless-powered communications: performance analysis and optimization," *IEEE Trans. Commun.*, vol. 63, no. 12, pp. 5178-5190, Dec 2015.
- [11] P.-T. Van, H.-H. N. Le, M.-D. N. Le, and D.-B. Ha, "Performance analysis in wireless power transfer system over Nakagami fading channels," in *2016 International Conference on Electronics, Information, and Communications (ICEIC)*, Jan 2016.
- [12] O. L. Alcaraz-López, H. Alves, R. D. Souza, and E. M. G. Fernández, "Ultrareliable short-packet communications with wireless energy transfer," *IEEE Signal Processing Letters*, vol. 24, no. 4, pp. 387-391, April 2017.
- [13] D. Kim, M. A. Ingram, and W. W. Smith, "Measurements of small-scale fading and path loss for long range RF tags," *IEEE Trans. Antennas Propag.*, vol. 51, no. 8, pp. 1740-1749, Aug 2003.
- [14] J. D. Griffin and G. D. Durgin, "Gains for RF tags using multiple antennas," *IEEE Trans. Antennas Propag.*, vol. 56, no. 2, pp. 563-570, Feb 2008.
- [15] N. O'Donoughue and J. M. F. Moura, "On the product of independent complex gaussians," *IEEE Trans. Signal Process.*, vol. 60, no. 3, pp. 1050-1063, Mar 2012.
- [16] M. Nakagami, "The m-distribution- a general formula of intensity distribution of rapid fading," *Statistical Method of Radio Propagation*, 1960.
- [17] M. K. Simon and M.-S. Alouini, *Digital Communication over Fading Channels*. Wiley-IEEE Press, 2005. [Online]. Available: <http://www.worldcat.org/isbn/0471649538>
- [18] Z. Wang and G. B. Giannakis, "A simple and general parameterization quantifying performance in fading channels," *IEEE Trans. Commun.*, vol. 51, no. 8, pp. 1389-1398, Aug 2003.
- [19] A. Bekkali, S. Zou, A. Kadri, M. Crisp, and R. V. Penty, "Performance analysis of passive UHF RFID systems under cascaded fading channels and interference effects," *IEEE Trans. Wireless Commun.*, vol. 14, no. 3, pp. 1421-1433, March 2015.
- [20] J. F. Paris, "Statistical characterization of  $\kappa$ - $\mu$  shadowed fading," *IEEE Trans. Veh. Technol.*, vol. 63, no. 2, pp. 518-526, Feb 2014.
- [21] S. L. Cotton, "Human body shadowing in cellular device-to-device communications: Channel modeling using the shadowed  $\kappa$ - $\mu$  fading model," *IEEE J. Sel. Areas Commun.*, vol. 33, no. 1, pp. 111-119, Jan 2015.
- [22] L. Moreno-Pozas, F. J. Lopez-Martinez, J. F. Paris, and E. Martos-Naya, "The  $\kappa$ - $\mu$  shadowed fading model: unifying the  $\kappa$ - $\mu$  and  $\eta$ - $\mu$  distributions," *IEEE Trans. Veh. Technol.*, vol. 65, no. 12, Dec 2016.
- [23] F. J. Lopez-Martinez, J. F. Paris, and J. M. Romero-Jerez, "The  $\kappa$ - $\mu$  shadowed fading model with integer fading parameters," *IEEE Trans. Veh. Technol.*, vol. PP, no. 99, pp. 1-1, 2017.

- [24] G. K. Karagiannidis, N. C. Sagias, and P. T. Mathiopoulos, “N\*Nakagami: a novel stochastic model for cascaded fading channels,” *IEEE Trans. Commun.*, vol. 55, no. 8, pp. 1453–1458, Aug 2007.
- [25] I. S. Gradshteyn and I. M. Ryzhik, *Table of Integrals, Series and Products*, 7th ed. Academic Press Inc, 2007.
- [26] A. Erdélyi, W. Magnus, F. Oberhettinger, and F. G. Tricomi, *Tables of Integral Transforms. Vol. I.* McGraw-Hill Book Company, Inc., New York-Toronto-London, 1954.
- [27] S. Bi, Y. Zeng, and R. Zhang, “Wireless powered communication networks: an overview,” *IEEE Wireless Communications*, vol. 23, no. 2, pp. 10–18, April 2016.
- [28] J. M. Romero-Jerez, F. J. Lopez-Martinez, J. F. Paris, and A. J. Goldsmith, “The fluctuating two-ray fading model: Statistical characterization and performance analysis,” *arXiv preprint arXiv:1611.05063*, 2016.
- [29] H. Stockman, “Communication by means of reflected power,” *Proceedings of the IRE*, vol. 36, no. 10, pp. 1196–1204, Oct 1948.
- [30] J. D. Griffin and G. D. Durgin, “Multipath fading measurements at 5.8 GHz for backscatter tags with multiple antennas,” *IEEE Trans. Antennas Propag.*, vol. 58, no. 11, pp. 3693–3700, Nov 2010.
- [31] K. Finkenzeller, *RFID Handbook: Fundamentals and Applications in Contactless Smart Cards, Radio Frequency Identification and Near-Field Communication*. John Wiley & Sons, 2010.
- [32] M. K. Simon, *Probability Distributions Involving Gaussian Random Variables: A Handbook for Engineers and Scientists*. Springer Science & Business Media, 2007.
- [33] M. Abramowitz and I. A. Stegun, *Handbook of Mathematical Functions: with Formulas, Graphs, and Mathematical Tables*. Courier Corporation, 1964, vol. 55.